

RFsheath heat flux estimates on Tore Supra and JET ICRF antennae. Extrapolation to ITER

L. Colas, Ph. Jacquet, G. Agarici, C. Portafaix, and M. Goniche

Citation: *AIP Conf. Proc.* **1187**, 133 (2009); doi: 10.1063/1.3273711

View online: <http://dx.doi.org/10.1063/1.3273711>

View Table of Contents: <http://proceedings.aip.org/dbt/dbt.jsp?KEY=APCPCS&Volume=1187&Issue=1>

Published by the [American Institute of Physics](#).

Related Articles

Properties of a warm plasma collisional sheath in an oblique magnetic field

Phys. Plasmas **19**, 113504 (2012)

Investigation of the sheath formation in a dusty plasma containing energetic electrons and nano-size dust grains

Phys. Plasmas **19**, 103505 (2012)

Potential contour shaping and sheath behavior with wall electrodes and near-wall magnetic fields in Hall thrusters

Phys. Plasmas **19**, 103502 (2012)

Spatio-temporal evolution and breaking of double layers: A description using Lagrangian hydrodynamics

Phys. Plasmas **19**, 102109 (2012)

The positive ion temperature effect in magnetized electronegative plasma sheath with two species of positive ions

Phys. Plasmas **19**, 102108 (2012)

Additional information on AIP Conf. Proc.

Journal Homepage: <http://proceedings.aip.org/>

Journal Information: http://proceedings.aip.org/about/about_the_proceedings

Top downloads: http://proceedings.aip.org/dbt/most_downloaded.jsp?KEY=APCPCS

Information for Authors: http://proceedings.aip.org/authors/information_for_authors

ADVERTISEMENT

AIPAdvances

Submit Now

**Explore AIP's new
open-access journal**

- **Article-level metrics
now available**
- **Join the conversation!
Rate & comment on articles**

RF-sheath heat flux estimates on Tore Supra and JET ICRF antennae. Extrapolation to ITER

L. Colas^a, Ph. Jacquet^b, G. Agarici^c, C. Portafaix^a, M. Goniche^a
and JET-EFDA contributors

^aCEA, IRFM, F-13108 Saint-Paul-lez-Durance, France.

^bEURATOM/UKAEA Fusion Association, Culham, OX14 3DB, UK

^cFusion for Energy, C/ Josep Pla 2, E-08019 Barcelona – Spain

Abstract. RF-sheath induced heat loads are identified from infrared thermography measurements on Tore Supra ITER-like prototype and JET A2 antennae, and are quantified by fitting thermal calculations. Using a simple scaling law assessed experimentally, the estimated heat fluxes are then extrapolated to the ITER ICRF launcher delivering 20MW RF power for several plasma scenarios. Parallel heat fluxes up to 6.7MW/m² are expected very locally on ITER antenna front face. The role of edge density on operation is stressed as a trade-off between easy RF coupling and reasonable heat loads. Sources of uncertainty on the results are identified.

Keywords: ICRF, RF-sheaths, particle convection, IR thermography, Tore Supra, JET, ITER.

PACS: 52.50.Qt, 52.35.Mw, 52.40.Fd, 52.40.Kh, 52.55.Rk, 44.10.+i, 44.40.+a

On several magnetic fusion devices, during additional heating of the plasma with waves in the Ion Cyclotron Range of Frequencies (ICRF), specific localized heat loads have been measured at extremities of open flux tubes around powered wave launchers [1-4]. They are generally attributed to radio-frequency (RF) sheath rectification [5]. To design the ITER ICRF antenna and neighbouring Plasma Facing Components (PFCs), it is important to estimate the magnitude of RF specific heat loads, for an adequate range of ITER Scrape-Off Layer (SOL) plasma conditions.

The present paper complements and benchmarks an earlier study based on pure modelling [6]. Here RF-sheath induced heat loads are first identified from infrared thermography measurements on Tore Supra (TS) ITER-like prototype (ILP) [7] and JET A2 antennae, and are quantified by fitting thermal calculations. Using a simple scaling law assessed experimentally, the estimated heat fluxes are then extrapolated to the ITER ICRF launcher delivering 20MW RF power on several plasma scenarios.

RF-SHEATH HEAT FLUX ESTIMATES ON TS AND JET

Infrared (IR) thermography diagnostics monitor the front faces of TS [8] and JET A2 ICRF antennae [9]. Several aspects of the IR measurements are exploited to estimate the heat fluxes quantitatively and ascertain their extrapolation to ITER. For a given antenna the magnitude of surface temperature elevation ΔT_{IR} is proportional to the applied heat flux. The areas of interest selected for analysis only heat up when the

* See the Appendix of F. Romanelli et al., Fusion Energy Conference 2008 (Proc. 22nd Int. FEC Geneva, 2008) IAEA, (2008)

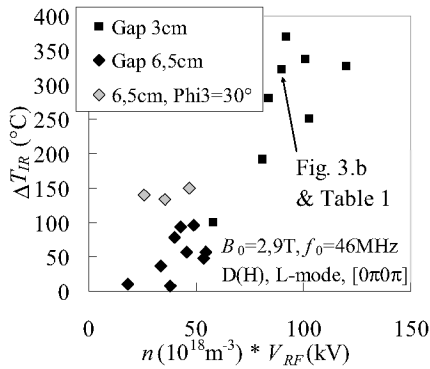


FIGURE 1. IR temperature elevation on JET antenna septum, 2s after RF switch-on, vs product of local plasma density by forward RF voltage in feeding lines, for several gaps antenna-separatrix.

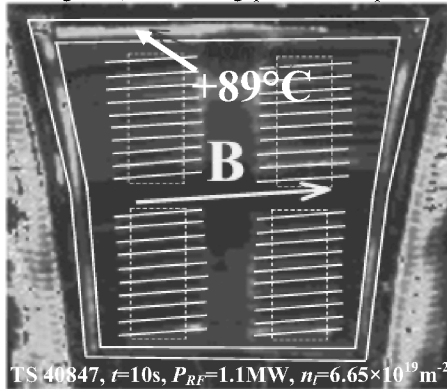
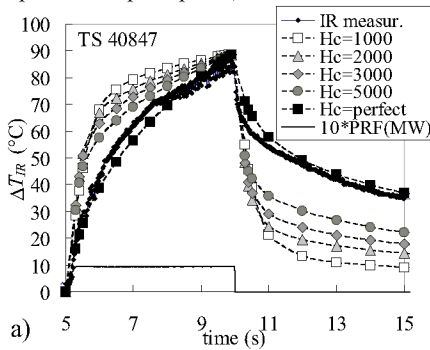


FIGURE 2. Surface temperature pattern measured with IR thermography during TS ILP operation. Superimposed, sketch of front face.



observed antenna is energized, thus identifying power fluxes specific of RF near fields. These zones include the frame of the TS ILP and the septum of JET A2 antennae. Over several pulses the core plasma density, the applied RF power and the radial gap to the separatrix were scanned. Figure 1 shows that on JET ΔT_{IR} is correlated with the product of antenna RF voltage with SOL density at $R=2.85\text{m}$ from Li beam, with some threshold that remains to be interpreted. Similar trends were recorded on TS [3] and are qualitatively consistent with RF-sheath theory [5]. JET IR data also suggest that heat fluxes increase when the toroidal strap phasing deviates from the standard $[0\pi 0\pi]$ (see also [10]). On figure 2 heat loads on TS ILP appear highly localized and asymmetric, with a maximum near the upper-left antenna box corner, in a region nearly tangent to the field lines. This observation as well as inhomogeneous interactions with a nearby Lower Hybrid wave launcher [11], suggest RF-induced local $\mathbf{E} \times \mathbf{B}$ density convection near upper and lower ILP frame [2].

Fitting $\Delta T_{IR}(t)$ with thermal calculation allows quantifying the heat fluxes Q_{\perp} normal to the antenna, provided that the front face thermal properties are known.

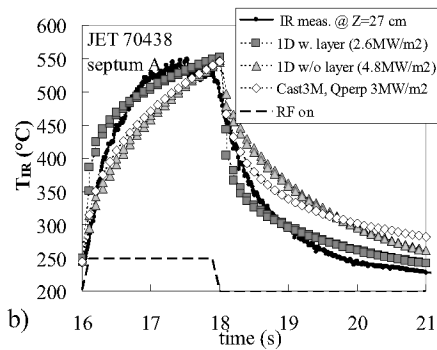


FIGURE 3. Fit of measured surface temperatures with thermal calculations and sensitivity studies to thermal properties. a) TS (fig.2), thermal contact H_c of B_4C coating; b) JET A2 case with surface layers.

Figure 3 illustrates how these properties can be inferred from $\Delta T_{IR}(t)$ rise and fall, assuming constant load during RF. In particular, as evidenced on JET divertor [12], JET time traces can only be fitted by including in the thermal model poorly adherent layers, whose characteristics remain loosely determined. These uncertainties, together with the imprecise localization of hot spots, complicate the quantification of JET heat fluxes. The main source of uncertainty on TS ($\sim 18\%$) is the IR emissivity of the B₄C antenna coating. Typical heat loads are listed on table 1. On TS parallel heat fluxes $Q_{||}$ were not deduced from Q_{\perp} , since TS fluxes are most probably *not* fully parallel to \mathbf{B}_0 .

EXTRAPOLATION EXERCISE TO ITER ICRF LAUNCHER

Following the simplest models in the literature [5], the extrapolation assumes that local RF-induced heat fluxes are proportional to both the local Bohm flux and the amplitude of RF currents developed by the antenna. This yields the parametric scaling

$$Q_{||} = \Gamma_{Bohm} e V_{DCsheath} \propto n (T_e + T_i)^{1/2} (P_{RF} / LR_c)^{1/2} \quad (1)$$

where n is the local density, T_e and T_i are local electron and ion temperatures, P_{RF} is the coupled RF power, L is the total length of radiating straps, and R_c is the coupling resistance per unit of strap length. Eq. (1) is qualitatively consistent with the observed parametric dependences (Figure 1, [3]), although it does not explicitly include RF-induced particle convection. In principle the DC sheath voltage amplitude involves the topology of RF current flows on all metallic structures [13], i.e. the detailed front face geometry [14] and the toroidal strap phasing (Figure 1, [3], [10]). In the present exercise, no geometrical effect is accounted for, i.e. the ITER launcher is formally replaced with 6 TS ILP or 3 A2 antennae, with the total strap length L rescaled to ITER values. To preserve the analogy with experiments, $[0\pi 0\pi]$ phasing was chosen for ITER strap array, a pessimistic option for RF coupling with a given density profile.

All RF and (unperturbed) plasma quantities involved in eq. (1) are measured on TS and JET or slightly extrapolated in the private SOL between antenna limiters. For ITER four cases of far SOL profiles were considered, corresponding to scenarios 2 and 4 in the central plasma [15]. For the first 4cm in the SOL, density profiles were calculated by B2-Eirene [16]. Beyond, two extrapolations were performed with different transverse transport coefficients, leading to short or long SOLs. Temperature profiles were assumed flat consistent with typical experimental profiles [17]. From these profiles, the RF coupling capabilities of the ITER launcher (april 2007 design) were estimated numerically with the antenna code TOPICA [18]. Table 1 shows that SOL densities cover 2 orders of magnitude, and correlatively R_c spans over a factor 3.

TABLE 1. RF-sheath peak heat fluxes extrapolated from TS and JET to ITER ICRF launcher using eq. (1), for 20MW coupled, $[0\pi 0\pi]$ toroidal strap phasing and four SOL plasma scenarios.

	TS 41176	JET 70438	Sc. 2 long	Sc. 4 long	Sc. 2 short	Sc. 4 short
P_{RF} (MW)	1.04	1.2	20	20	20	20
LR_c (Ω)	1.21	35.2	44.24	16.54	17.99	13.13
T_e (eV) mouth	10	20	11.7	23	11.7	23
T_i (eV) mouth	20	40	21.6	59	21.6	59
n (m ⁻³) mouth	4.2×10^{17}	2.5×10^{18}	1.1×10^{18}	6.0×10^{17}	5.2×10^{15}	3.9×10^{15}
Q_{\perp} (MW/m ²)	0.4	1.6	1.4/1.9	1.8/2.7	0.01/0.016	0.014/0.02
$Q_{ }$ (MW/m ²)	?	4	4.8	6.7	0.04	0.05

Table 1 summarizes the extrapolated heat fluxes. Most pessimistic expectations from TS yield $Q_{\perp} \sim 1.8 \text{ MW/m}^2$ locally, and from JET $Q_{\parallel} \sim 6.7 \text{ MW/m}^2$. Extrapolated results are ~ 1.9 - 2.4 times lower than peak fluxes inferred from modelling with ITER 2007 geometry [6]. Both modeling and observations suggest that these peak fluxes are highly localized spatially. Despite lower DC sheath voltages, “long SOL” profiles produce these highest heat fluxes, due to higher local density at the antenna mouth.

CONCLUSIONS AND OUTLOOK

This work allowed both identifying experimentally RF sheath effects as a source of heat loads on JET and ascertaining scaling laws for extrapolation. Quantitative heat fluxes cover a wide range. Several sources of uncertainty were identified, attributed to 1°) error bars on IR and SOL measurements; 2°) poorly known thermal properties; 3°) simple extrapolation models; 4°) RF-induced density modifications neglected; 5°) antenna geometry effect not accounted for; 6°) poor knowledge of ITER SOL profiles.

Parametric scaling with n and V_{RF} was evidenced. Competition between these two parameters explains the variations of extrapolated heat loads with the plasma scenario: as already experienced on TS [19], optimal ICRF antenna operation might result from a trade-off between reasonable RF wave coupling (critical for short SOLs) and tolerable heat loads (critical for long SOLs). Depending on the actual ITER SOL, the trade-off might be resolved by adapting the radial gap to the separatrix, as on figure 1. Besides, RF sheaths could be reduced by optimizing the RF current flows on antenna front face, without necessarily degrading the wave coupling properties [10], [14].

Acknowledgements. This work, supported by the European Communities under the contract of Association between EURATOM and CEA, was carried out within the framework of the contract EFDA 07/1700-1572. The views and opinions expressed herein do not necessarily reflect those of the European Commission.

REFERENCES

1. T. Imai, H. Sawada, Y. Uesugi, S. Takamura, *Journal Nucl. Materials* **266-269** (1999) p.969
2. M. Bécoulet, et al. *Phys. Plasmas*, **Vol. 9**, No. 6, pp. 2619-2632, June 2002
3. L. Colas et al., *Nuclear Fusion*, vol.**46**, pp. S500-S513 (2006)
4. K. Saito et al. *Journal of Nuclear Materials* **363-365** (2007) pp. 1323-1328
5. Perkins F.W., *Nuclear Fusion* **29** (4) 1989, p. 583
6. L. Colas et al., *JNM* **390-391** (2009) 959-962; full report: CEA note PHY-NTT/2008.008
7. K. Vulliez et al. *Nuclear Fusion*, **48**, 065007 (2008) and A. Argouarch et al., this conference
8. D. Guilhem et al. *Fusion Engineering and Design*, vol. **74**, p. 879-883 (2005).
9. E. Gauthier et al., Proc. 24th SOFT, Warsaw (2006), *Fus. Eng. & Des.* **82** (2007) 1335-1340
10. V.V. Bobkov et al., this conference
11. A. Ekedahl, A. Mendes, L. Colas, J. Hillairet and K. Vulliez, this conference
12. P. Andrew et al., *Journal of Nuclear Materials* **313-316** (2003) 135-139.
13. L. Colas, S. Heuraux, S. Brémond, G. Bosia, *Nuclear Fusion*, Vol. **45** (2005), p. 767-782
14. A. Mendes, L. Colas, K. Vulliez, A. Ekedahl, A. Argouarch, D. Milanese, this conference
15. A. Loarte et al., Proc. 22nd Fusion Energy Conference, IAEA, (Geneva 2008) IT/P6-13
16. R. Schneider, X. Bonnin, et al., *Contribution Plasma Phys.* **46** (2006) 3
17. B. Lipschultz et al., *Nuclear Fusion* **47** No 9 (September 2007) 1189-1205
18. V. Lancellotti et al., *Nuclear Fusion* **46** (2006) S476
19. A. Ekedahl et al., Proc. 17th Top. RF Conf. Clearwater (Fl) 2007, AIP CP **933**, pp. 237-244